

Dataset Bias in Few-shot Image Recognition

Shuqiang Jiang, *Senior Member, IEEE*, Yaohui Zhu, Chenlong Liu,
Xinhang Song, Xiangyang Li, and Weiqing Min

Abstract—The goal of few-shot image recognition (FSIR) is to identify novel categories with a small number of annotated samples by exploiting transferable knowledge from training data (base categories). Most current studies assume that the transferable knowledge can be well used to identify novel categories. However, such transferable capability may be impacted by the dataset bias, and this problem has rarely been investigated before. Besides, most of few-shot learning methods are biased to different datasets, which is also an important issue that needs to be investigated deeply. In this paper, we first investigate the impact of transferable capabilities learned from base categories. Specifically, we use the relevance to measure relationships between base categories and novel categories. Distributions of base categories are depicted via the instance density and category diversity. The FSIR model learns better transferable knowledge from relevant training data. In the relevant data, dense instances or diverse categories can further enrich the learned knowledge. Experimental results on different sub-datasets of ImageNet demonstrate category relevance, instance density and category diversity can depict transferable bias from distributions of base categories. Second, we investigate performance differences on different datasets from the aspects of dataset structures and different few-shot learning methods. Specifically, we introduce image complexity, intra-concept visual consistency, and inter-concept visual similarity to quantify characteristics of dataset structures. We use these quantitative characteristics and eight few-shot learning methods to analyze performance differences on five different datasets (i.e., MiniCharacter, MiniImageNet, MiniPlaces, MiniFlower, MiniFood). Based on the experimental analysis, some insightful observations are obtained from the perspective of both dataset structures and few-shot learning methods. We hope these observations are useful to guide future few-shot learning research on new datasets or tasks. Our data is available at <http://123.57.42.89/dataset-bias/dataset-bias.html>.

Index Terms—Few-shot image recognition, meta-learning, knowledge transfer, dataset bias

1 INTRODUCTION

LEARNING from few examples and generalizing to different situations are capabilities of human visual intelligence. During the past years, significant progress has been made on image recognition [1], [2], [3] with the assistance of deep learning techniques [4] and large scale labelled dataset [5], [6]. However, this kind of human visual intelligence is yet to be matched by leading machine learning models. Humans can easily learn to recognize a novel object category after glancing at only one or a few examples [7]. This cognitive ability can be explained by the "learning to learn" mechanism in the brain [8], which means that human can make inference so that their previously acquired knowledge on related tasks can be flexibly adapted to a new task. Inspired by this human ability, the few-shot image recognition (FSIR) is proposed to learn novel concepts from a few, or even a single example.

The task of FSIR establishes a new recognition setup to transfer the knowledge of training tasks sampled from training (base) categories to the new task with one or very few samples. Instead of learning one single recognition task, most FSIR models learn plenty of recognition tasks. Each task contains a support set (training samples) and a target set (test samples). The support set consists of a few available labelled data, which is exploited to learn a task-specific model. Then the learned model is evaluated on the target

set. Each task in these two sets shares the same concepts. But concepts of testing tasks come from novel categories, which are different from those of training tasks.

Current studies of FSIR [9], [10], [11], [12], [13], [14], [15] achieve transferable knowledge by learning training tasks or base categories. These studies mostly focus on transferable knowledge between datasets or tasks by exploiting given base categories. The majority of current works assume the transferable knowledge globally shared across all tasks, and consider that the learned knowledge can be well adapted to novel categories. However, transferable knowledge is highly dependent on the distributions of base categories. FSIR models can acquire biased transferable capabilities if distributions of base categories and novel categories are very different. Furthermore, current studies rarely explore the characteristics of dataset structures, which include not only an amount of information in the image but also semantic gaps between original images and concepts. Current works do not deeply dig differences in dataset structures. Therefore, current few-shot learning methods may be biased to different datasets.

Two problems arise based on the above analysis: i) What factors can describe transferable bias from distributions of base categories? ii) What characteristics can depict bias of few-shot learning methods on different datasets? In this paper, we focus on studying these two problems systematically, which have rarely been explored before. Fig. 1 (a) illustrates the investigation of the first problem, and Fig. 1 (c) illustrates the investigation of the second problem.

For the first problem, we aim to obtain transferable knowledge from base categories, which can be better adapted to novel categories. The FSIR model can learn

• The authors are with the Key Laboratory of Intelligent Information Processing of Chinese Academy of Sciences (CAS), Institute of Computing Technology, CAS, Beijing 100190, China and also with the University of Chinese Academy of Sciences, Beijing 100049, China.
E-mail: sqjiang@ict.ac.cn, [yaohui.zhu, chenlong.liu, xinhang.song, xiangyang.li](mailto:{yaohui.zhu, chenlong.liu, xinhang.song, xiangyang.li}@vip.ict.ac.cn)

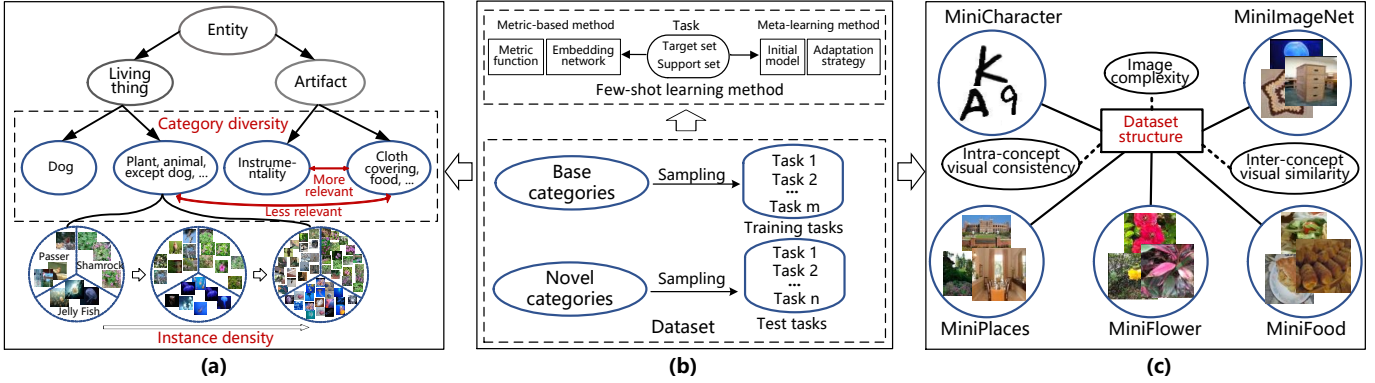


Fig. 1. The two investigations for FSIR from the dataset. (a): illustrations of dataset diversity. (b): illustrations of the few-shot learning tasks sampled from datasets and the few-shot learning method. (c): illustrations of dataset structures.

more accurate knowledge from dense instances, more comprehensive knowledge from diverse categories, especially, transferable capabilities from relative categories. Therefore, we introduce the dataset diversity to depict distributions of base categories and the relevance to measure relationships between base categories and novel categories. The dataset diversity contains instance density and category diversity. We conduct experiments on eight few-shot learning methods, which contains four classic methods such as Prototypical Net [9], MAML [13], and four recent methods. We measure relevance of categories contained in ImageNet [16] both qualitatively and quantitatively to obtain different sub-datasets which contain dense instances and diverse categories. Under the settings of different relevance, instance density and category diversity are explored respectively. Besides, we further compare instance density and category diversity with the fixed number of total samples.

For the second problem, we aim to analyze differences in performance on different datasets from characteristics of dataset structures and different few-shot learning methods (e.g., metric-based methods and meta-learning methods shown in Fig. 1 (b)). We introduce image complexity, intra-concept visual consistency, and inter-concept visual similarity to quantify characteristics of dataset structures. To conduct comprehensive evaluations on multiple datasets, we introduce five datasets, including simple character images (i.e., MiniCharacter), images with different number of objects (i.e., MiniImageNet, MiniPlaces), and two fine-grained datasets (i.e., MiniFlower and MiniFood). We use five kinds of features to calculate intra-concept visual consistency and inter-concept visual similarity, and measure image complexity in two manners. These quantitative characteristics are used to analyze differences in performance on different datasets. In addition, we give analysis on differences in performance of these few-shot learning methods.

In summary, our main contributions are as follows: i) We systematically investigate the influence of knowledge learned from base categories. ii) We systematically investigate differences in performance on different datasets with three characteristics of dataset structures and two types of few-shot learning methods. iii) Based on the above investigations, we can obtain following key conclusions:

- The FSIR model can obtain better performance with knowledge learned on relevant base categories rather

than irrelevant ones.

- The FSIR model can obtain improvement with knowledge learned on more dense instances or diverse categories without reducing the relevance.
- The FSIR model can obtain more improvements with knowledge learned on diverse categories than that learned on dense instances without reducing the relevance, when there are enough instances for each category.
- The FSIR model obtains different performance on different datasets, which can be depicted with image complexity, intra-concept visual consistency, and inter-concept visual similarity.
- Different FSIR models have diverse performance on different datasets, which is relevant to both dataset structures and the method ability. The method ability is closely related to characteristics of dataset structures.

The remainder of this paper is constructed as follows. Sect. 2 provides the related work, including FSIR, domain adaptation, and few-shot domain adaptation. Sect. 3 gives formulation of FSIR and reviews two types of classic few-shot learning methods. Sect. 4 presents evaluations of the dataset diversity in detail. Sect. 5 presents evaluations of the dataset structure and experimental analysis in detail. Sect. 6 provides some perspectives and future directions. Finally, the paper closes with conclusions in Sect. 7.

2 RELATED WORK

2.1 Few-shot Image Recognition

The goal of FSIR is to identify novel categories with a few annotated examples and knowledge obtained from base categories. In early attempts, Fei-Fei *et al.* [17] propose a variational bayesian framework for one-shot image classification, and Lake *et al.* [18] propose hierarchical bayesian program learning on the few-shot alphabet recognition tasks. Inspired by architectures with augmented memory capacities such as Neural Turing Machines (NTMs), Santoro *et al.* [19] propose a meta-learning method with memory-augmented neural networks. Afterwards, there are three kinds of methods to deal with the FSIR problem. The first one is metric-based method (i.e., learning to compare),

which learns a transferable embedding network or function. This function transforms the original images into the embedding space such that these images can be recognized with a nearest neighbor [20], [21], a linear classifier [9], [22], [23] or a deep nonlinear metric [10]. The second one is meta-learning method [12], [24], [25] (i.e., learning to learn), whose learning occurs at two levels: task-level learning and take-specific adaption. The task-level learning is usually implemented by an additional meta-learner [14], [26] or a sensitive initialization shared with task-specific learners [13], [27], which can provide meta-level information for the take-specific adaption. The third method is generative or augmentation-based method (i.e., learning to generate or augment), which learns a generative model to synthesize more samples and then trains a robust classifier. This generative model uses semantic information [28], [29] (e.g., attribute), or base categories for analogy or hallucination [30], [31].

Recently, some works study FSIR from the view of self-supervised approaches [32], [33] and semi-supervised approaches [34], [35]. Yu *et al.* [36] propose a two-stage approach which explores knowledge from both annotated examples of base categories and un-annotated ones of novel categories. The above works focus on learning transferable knowledge with given datasets. However, we investigate the performance of FSIR from dataset diversity with changeable base categories and different characteristics of dataset structures. A more related work is [37], which shows that increasing relevant categories in close or far semantic distances can boost the performance of FSIR. In addition, our work also considers increasing irrelevant categories, and experimental results illustrate that more irrelevant categories cannot improve the performance, suggesting that it's not the more categories the better performance. Furthermore, we investigate differences in performance on different datasets from the dataset structure and different few-shot learning methods, which is not explored by [37].

2.2 Domain Adaptation

Domain adaptation utilizes labeled data in one or more relevant source domains to execute new tasks in a target domain with scarce annotated data. It aims to solve the domain gap and transfer knowledge learned on the source domain to the target domain [38], [39], [40], [41]. As many approaches are based on deep neural networks, Li *et al.* [42] construct source and target datasets with various distances to analyze factors that affect the effectiveness of using prior knowledge from a pre-trained model with a fixed network architecture. Azizpour *et al.* [43] investigate factors (e.g., network architectures, parameters of feature extraction) affecting the transferability of feature representations in generic convolutional networks. To learn domain invariant features minimizing the domain discrepancy, Long *et al.* [44] propose a deep network architecture that can jointly learn adaptive classifiers and transferable features from labeled data in the source domain and unlabeled data in the target domain. Meanwhile, with significant advances made in image synthesis by generative adversarial networks, many methods focus on learning domain-independent features and synthesizing examples in the new domain [45], [46]. Hoffman *et al.*

[47] propose adversarial learning method that utilizes both generative image space alignment and latent representation space alignment. Zhang *et al.* [48] propose an adversarial learning method with two-level domain confusion losses. Cui *et al.* [49] propose gradually vanishing bridge mechanism to learn more domain-invariant representations. To tackle predictive domain adaptation, Mancini *et al.* [50] leverage meta data information to build a graph and design novel domain-alignment layers based on the graph for domain adaption. These works have the same classes among different domains. However, we address the problem in FSIR, where the classes in target domain are disjoint with ones in source domains. Meanwhile, the training examples in the target domain are limited or rare.

2.3 Few-shot Domain Adaptation

Few-shot domain adaptation aims to recognize novel categories with a few annotated data in the target domain and sufficient data in the source domains. Some works [51], [52] assume that the target domain contains the same classes as the source domain. Recently, some efforts attempt to address a more flexible and challenging few-shot domain adaptation, where the target domain and source domains have disjoint classes, called cross-domain few-shot learning. Chen *et al.* [11] evaluate current models and proposed baselines on cross-domain few-shot protocols (from MiniImageNet [22] to cub [53]). Tseng *et al.* [54] propose a learned feature-wise transformation to stimulate feature distributions cross domains with a small number of samples. Guo *et al.* [55] introduce a more realistic cross-domain few-shot learning, where the source domain consists of common images from Imagenet [16], and the target domains contain rare images such as satellite images and radiological images. Besides, Vuorio *et al.* [56] propose the multi-domain few-shot learning, and use a task-aware modulation to promote the learning of meta-learner. Yao *et al.* [57] propose a hierarchically structured meta-learning algorithm to promote knowledge customization on different domains but simultaneously preserve knowledge generalization in related domains. Triantafyllou *et al.* [27] introduce a meta-dataset that consists of 10 datasets in different domains and present experimental evaluation of current models and proposed baselines. These works only use given source domains without selections, in contrast, we selectively use source domains (i.e., base categories) and systematically investigate different target domains from characteristics of dataset structures and different few-shot learning methods.

3 PRELIMINARIES

3.1 Few-shot Image Recognition Formulation

In the regular machine learning setting, a classification problem is defined on instances $\mathcal{I}_{(x,y)} \sim p(\mathcal{I})$, where x is a sample and y is the corresponding label. But most FSIR models learn task instances $\mathcal{T} \sim p(\mathcal{T})$. Sampling from training and test data, we form training tasks \mathcal{T}^{train} and testing tasks \mathcal{T}^{test} , respectively. According to existing settings, the training and test data are made of base and novel categories, respectively, and each category has plenty of samples. For example, in MiniImageNet [22], the number

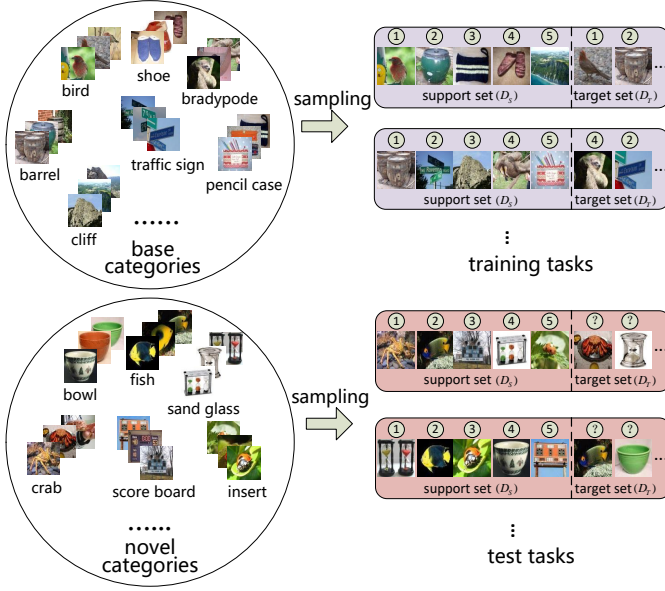


Fig. 2. The training and test tasks are formed by randomly sampling from the base and novel categories, respectively.

of base and novel categories are 64 and 20 respectively, where each category has 600 samples.

In training tasks \mathcal{T}^{train} or testing tasks \mathcal{T}^{test} , each task is defined as $\mathcal{T}_j = \{D_{\mathcal{T}_j,S}, D_{\mathcal{T}_j,T}\}$, where $D_{\mathcal{T}_j,S}$ is a support set (training samples) and $D_{\mathcal{T}_j,T}$ is a target set (test samples). The support set $D_{\mathcal{T}_j,S} = \{(x_c^k, y_c^k) \mid c = 1, 2, \dots, C; k = 1, 2, \dots, K\}$ and the target set $D_{\mathcal{T}_j,T}$ consist of C categories randomly sampled from the total categories, and each sampled category contains K labeled samples in the support and some samples in the target set. And this task is called C -way K -shot task. Test tasks \mathcal{T}^{test} and training tasks \mathcal{T}^{train} have the same form but with disjoint label space since they have different categories. Fig. 2 illustrates the 5-way 1-shot training and test tasks, which are sampled from base and novel categories, respectively.

3.2 Few-shot Learning Methods

Metric-based methods and meta-learning methods are employed to explore the dataset bias. These two kinds of methods do not use additional information and are easy to be implemented with less options, compared with generative or augmentation-based methods. In the following, we introduce the typical works in these two kinds of methods.

3.2.1 Metric-based Methods

This kind of method contains two parts: an embedding network or function $\mathcal{G}()$ and a metric function $\mathcal{M}()$. A key assumption is that $\mathcal{G}()$ learns domain-general information as an inductive bias [58] to generalize novel categories. In addition, the learning target or the loss function $\mathcal{L}()$ affects $\mathcal{G}()$ learning (or $\mathcal{M}()$ learning, when $\mathcal{M}()$ is parameterized). Hence, we review the following metric-based few-shot learning methods from $\mathcal{L}()$ and $\mathcal{M}()$.

Prototypical Net (PN) [9]. In this method, the $\mathcal{M}()$ is the Euclidean distance function. The $\mathcal{L}()$ is the cross entropy

loss, and the probability of each sample in D_T is defined as (omitting the index of task):

$$P(\bar{y}|\bar{x}, D_S) = \frac{e^{-\mathcal{M}(\mathcal{G}(\bar{x}), \sum_{(x,y) \in D_S} \mathbf{I}\{y=\bar{y}\} \mathcal{G}(x))}}}{\sum_{a=1}^{a=C} e^{-\mathcal{M}(\mathcal{G}(\bar{x}), \sum_{(x,y) \in D_S} \mathbf{I}\{y=y_a\} \mathcal{G}(x))}} \quad (1)$$

where C is the number of way, K is the number of shot and $(\bar{x}, \bar{y}) \in D_T$.

Relation Network (RN) [10]. This method learns a parameterized $\mathcal{M}()$, which is implemented by a neural network. The $\mathcal{L}()$ is mean square error, defined as:

$$\mathcal{L}() = \sum_{(\bar{x}, \bar{y}) \in D_T} \sum_{(x,y) \in D_S} (r(\bar{y}|\bar{x}, D_S) - \mathbf{I}\{y = \bar{y}\})^2 \quad (2)$$

where $r(\bar{y}|\bar{x}, D_S) = \mathcal{M}(\mathcal{G}(\bar{x}), \text{pooling}(\{\mathcal{G}(x) \mid (x,y) \in D_S, y = \bar{y}\}))$, and the $\text{pooling}()$ is maxpooling in [10].

Deep Subspace Networks (DSN) [23]. In this method, the $\mathcal{M}()$ is implemented with task-adaptive subspace metrics, i.e., $\{\mathcal{M}_{y_a}(\bar{x})\}_{a=1}^C$. The $\mathcal{L}()$ is the cross entropy loss, and the probability of each sample in D_T is defined as:

$$P(\bar{y}|\bar{x}, D_S) = \frac{e^{-\mathcal{M}_{\bar{y}}(\bar{x})}}{\sum_{a=1}^{a=C} e^{-\mathcal{M}_{y_a}(\bar{x})}} \quad (3)$$

where $\mathcal{M}_{y_a}(\bar{x}) = -\|(\mathbf{I} - P_{y_a} P_{y_a}^T)(\mathcal{G}(\bar{x}) - u_{y_a})\|^2$, P_{y_a} is a matrix with orthogonal basis for the linear subspace spanning $X_a = \{\mathcal{G}(x) \mid y = y_a, (x,y) \in D_S\}$, $u_{y_a} = \frac{1}{K} \sum_{x \in X_a} \mathcal{G}(x)$, and $(\bar{x}, \bar{y}) \in D_T$

DEMD [21]. In this method, the Earth Mover's Distance (EMD) is to obtain optimal matching flows $\tilde{\mathcal{M}}()$ between each two feature maps $\mathcal{G}()$. Thus the similarity metric between two maps is $\mathcal{M}() = \text{Cos}(\tilde{\mathcal{M}}())$, where $\text{Cos}()$ is cosine similarity of two vectors in the maps. The $\mathcal{L}()$ is the cross entropy loss, and the probability of each sample in D_T is defined as:

$$P(\bar{y}|\bar{x}, D_S) = \frac{e^{-\mathcal{M}(\mathcal{G}(\bar{x}), \sum_{(x,y) \in D_S} \mathbf{I}\{y=\bar{y}\} \mathcal{G}(x))}}}{\sum_{a=1}^{a=C} e^{-\mathcal{M}(\mathcal{G}(\bar{x}), \sum_{(x,y) \in D_S} \mathbf{I}\{y=y_a\} \mathcal{G}(x))}} \quad (4)$$

where $(\bar{x}, \bar{y}) \in D_T$.

3.2.2 Meta-learning Methods

This kind of method usually contains two parts: an initial model $\mathcal{F}(); \theta$ and an adaptation strategy $\mathcal{S}(); \delta$, where θ are parameters of $\mathcal{F}()$, and δ are parameters of $\mathcal{S}()$. The processes of this kind of method are: i) computing the gradient (or loss) information on support set: $\text{grad}_{a_t/\theta} = \nabla_{a_t/\theta} \mathcal{L}(\mathcal{F}(D_S(x); \theta), D_S(y))$, where $\mathcal{L}()$ is the loss function, a_t is the t^{th} neurons of $\mathcal{F}()$; ii) transforming the gradient information into adaptive information: $I = \mathcal{S}(\text{grad}; \delta)$; iii) leveraging the adaptive information to obtain an updated model: $\mathcal{B}(\mathcal{F}(); \theta, I)$. Similarly, we review the following meta-learning methods from the $\mathcal{S}()$. Generally speaking, the final learning target or the loss function calculated on the target set has the same formulation as $\mathcal{L}()$ mentioned in the ii) process.

Model-Agnostic Meta-Learning (MAML) [13]. This method is inspired by fine-tuning. It computes gradient of the whole parameter θ , and then directly uses the gradient

on original parameters with one or a few gradient steps to obtain the updated model: $\mathcal{B}(\mathcal{F}(\cdot;\theta), I) = \mathcal{F}(\cdot; \theta - r \cdot I)$, where $I = \text{grad}_\theta$, r is updating learning rate.

Proto-MAML [27]. As a variant of MAML, this method also updates the whole parameter θ for adaptation. Different from MAML, the classifier weight of Proto-MAML is initialized with the prototype of classes [9]. The classifier weight initialization can be formed as $\theta_c := \mathcal{F}(D_S(x); \theta_e)$, where θ_c and θ_e are parameters of the classifier and the embedding network, respectively. The gradient on support set is achieved via $\text{grad}_\theta = \nabla_\theta \mathcal{L}(\mathcal{F}(D_S(x); \{\theta_e, \theta_c\}), D_S(y))$, where $\theta = \{\theta_e, \theta_c\}$. Thus the updated model is $\mathcal{B}(\mathcal{F}(\cdot;\theta), I) = \mathcal{F}(\cdot; \theta - r \cdot \text{grad}_\theta)$, where r is updating learning rate.

adaCNN [14]. This method computes gradient of neurons $\text{grad}_t = \nabla_{a_t} \mathcal{L}(\mathcal{F}(D_S(x); \theta), D_S(y))$, and transforms the gradient into conditional shift vectors $\beta_{t,m} = I_{m,t} = S(\text{grad}_{a_t,m}; \delta)$ (m is the m^{th} instance in the support set) that are saved in a memory. The updated model is as follows:

$$\mathcal{B}(\mathcal{F}(\cdot;\theta), \beta_t) = \begin{cases} \sigma(\mathcal{F}(a_t;\theta)) + \sigma(\beta_t) & t \neq T \\ \text{softmax}(\mathcal{F}(a_t;\theta) + \beta_t) & t = T \end{cases} \quad (5)$$

where T is the final layer, $\sigma(\cdot)$ is a nonlinear function, and $\text{softmax}(\cdot)$ is the Softmax function. The layer-wise shifts are recalled from memory via a soft attention to obtain β_t ($\beta_t = \sum_m w_m \beta_{t,m}$, w_m is calculated by a key function), which is used for adjusting the output of initial model.

MetaOpt [12]. This method learns an adaptive classifier for adaptation. The classifier is implemented with SVM, which can be solved by optimizing a convex objective function. The weight of the adaptive classifier is achieved via $\theta_c^* := \underset{\theta_c}{\text{argmin}} \mathcal{L}(\mathcal{F}(D_S(x); \{\theta_e, \theta_c\}), D_S(y))$, where θ_c^* and θ_e are parameters of the adaptive classifier and the embedding network, respectively. Thus the updated model is $\mathcal{B}(\mathcal{F}(\cdot;\theta), I) = \mathcal{F}(\cdot; \{\theta_e, \theta_c^*\})$.

3.2.3 Summary

Metric-based methods do not need task-specific adaptation. They require data with a high relevance between base categories and novel categories especially for a learnable metric. Metric-based methods focus on designing an effective metric. For the above four metric-based methods, two of them are classic, another two are up to date. In the two classic method, PN uses a predefined metric, and RN utilizes a parametric network as the metric. In the two recent works, DSN adopts task-adaptive subspace metrics, and DEMD measures each two images with the Earth Mover’s Distance. Therefore, the four metric-based methods have their characteristics in the metric function.

Compared with metric-based methods, meta-learning methods update their models via task-specific adaptation, such that these methods are less dependent on the relevance. For the above four meta-learning methods, MAML is the classic one, which updates the whole weights of the initial network for adaption. Different from the MAML, adaCNN updates activations for adaption. Proto-MAML is a variant of MAML, and initializes classifier weight with the prototype of classes. For adaption, the three meta-learning methods update the whole weight or some activations of

network. In contrast, MetaOpt only updates task-sensitive classifier. Therefore, the four meta-learning methods have their characteristics in the model initialization or the designing of adaptation strategy.

We use the eight representative few-shot learning methods (i.e., four metric-based methods and four meta-learning methods) to carry out experiments on diverse datasets to analyze dataset bias of FSIR in the following sections.

4 EVALUATION OF DATASET DIVERSITY

The FSIR model aims to recognize novel categories with a small amount of samples by exploiting learnable generic knowledge. This kind of knowledge is learned from sufficient base categories, whose diversity can explicitly affect the quality of the learned knowledge. In this section, we study dataset diversity of base categories to explore FSIR. First, we introduce some key factors of dataset diversity. Second, we present evaluated datasets and settings. Next, we explore these factors independently and compare them. Finally, we give some discussions.

4.1 Factors of Dataset Diversity

The dataset diversity can be reflected in two aspects including instance density and category diversity. On one hand, dense instances can provide each concept with lots of variations in pose, scale, illumination, distortion, background, etc. Thus the FSIR model can learn more accurate knowledge from dense instances. On the other hand, diverse categories can provide plenty of concepts with larger visual difference. Thus the FSIR model can learn more comprehensive knowledge from diverse categories.

4.2 Datasets and Settings

As ImageNet [16] is a well-known large dataset which has been widely used for both visual recognition and FSIR (e.g., MiniImageNet [22]), we construct different subsets which contain dense instances and diverse categories for FSIR. We use the ImageNet (ILSVRC2012) dataset with 1000 categories and 1.28 million images. Each category corresponds to one synset in WordNet [59]. We find its parent synsets recursively until reaching the node of entity which is the root of the WordNet, according to their hierarchical semantic relations. In this manner, we can obtain the entire tree structure of the 1000 categories, which are divided into different branches with different relevance.

The branches of the 1000 categories are illustrated in Fig. 3. All categories belong to the entity branch, as the entity node is the root of the tree structure. And they are divided into two branches according to whether they are man-made or nature. More precisely, as shown in Fig. 3, the first one is living thing branch which contains 451 categories, and the second one is artifact branch which contains 549 categories. The living thing branch is further divided into the dog branch (which contains various dogs, denoted as DOG) and the LTED (which is the short for Living Thing Except Dog) branch which is the rest of the living thing branch except the categories in the dog branch. Meanwhile, the artifact branch is divided into the ARIN (which is short for ARtifact INstrument) branch which is the super class of

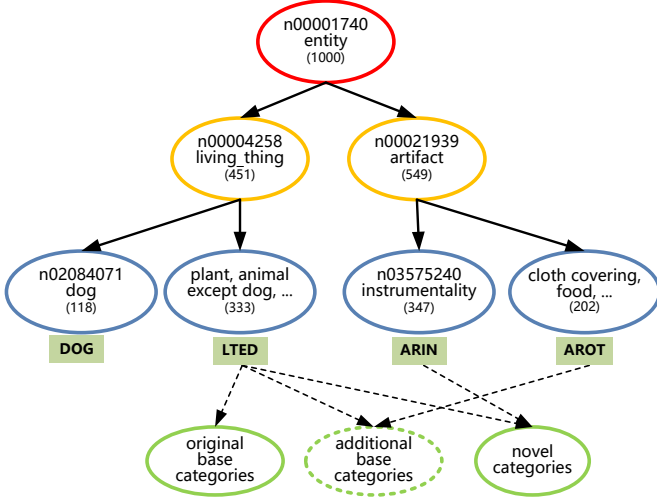


Fig. 3. The hierarchical display of the 1000 categories in ImageNet. The integer in the parenthesis indicates the number of the categories that the branch contains. The number in the beginning of the node is the corresponding WordNet ID. The LTED, ARIN and AROT are three branches, which are sampled to form original (additional) base and novel categories.

instrumentality and the AROT (which is short for ARtifact Other Thing) branch which is the rest of the artifact branch.

To qualitatively measure the relevance between different categories, we utilize the approaches used in [42], [60] to estimate their relevance, according to the tree structure of ImageNet. The categories in the same branch are more relevant than the ones in other different branches. For example, as the categories in the LTED branch contain animals such as cat, sheep, kangaroo, while categories in the ARIN branch contain many traffic instruments, the base networks trained on some categories belonging to LTED have features which will help classify some other categories in LTED branch. So the categories in the LTED branch are more relevant to each other compared to the categorizes in the other branches.

Meanwhile, measuring the relevance between different datasets quantitatively is complementary to the qualitative analysis, and it can distinguish different datasets more clearly and accurately. So we utilize Word Mover’s Distance (WMD) [61], [62] and Shortest Path Length (SPL) [59], [63], [64] to measure their relevance quantitatively. Specifically, a small distance means a great relevance.

- **WMD:** the WMD distance originally measures the dissimilarity between two text documents as the minimum amount of distance that the embedded words of one document need to travel to reach the embedded words of another document. Recently, it has been proposed for distributional metric matching and applied to cross-domain alignment. In the same spirit of the approach used in [62], we use WMD to measure the relevance between two sets of entities. Let \mathbb{D}_x and \mathbb{D}_y represent two sets of categories (i.e., entities) from two different datasets. As each category in the data corresponds to one synset in WordNet, we utilize the corresponding text to represent each category. In this way, \mathbb{D}_x and \mathbb{D}_y are denoted as $\tilde{X} = \{\tilde{x}_i\}_{i=1}^n$ and $\tilde{Y} = \{\tilde{y}_i\}_{i=1}^m$ respectively, where n

TABLE 1
Distances between different datasets which are obtained with the metric of WMD.

	DOG	LTED	ARIN	AROT
DOG	0	3.1981	3.5829	3.5438
LTED	3.1981	0	3.5102	3.4782
ARIN	3.5829	3.5102	0	3.3787
AROT	3.5438	3.4782	3.3787	0

TABLE 2
Distances between different datasets which are obtained by the metric of SPL according to the tree structure of WordNet.

	DOG	LTED	ARIN	AROT
DOG	0	13.39	19.60	18.97
LTED	13.39	0	16.12	15.40
ARIN	19.60	16.12	0	10.80
AROT	18.97	15.40	10.80	0

and m are the number of categories in each dataset and \tilde{x}_i and \tilde{y}_i are the corresponding words. The distance between \mathbb{D}_x and \mathbb{D}_y is obtained by computing the dissimilarity between \tilde{X} and \tilde{Y} with the WMD metric, denoted as $\mathcal{D}_{wmd}(\mathbb{D}_x, \mathbb{D}_y) = WMD(\tilde{X}, \tilde{Y})$. Here we utilize the word2vec [65] embedding to represent each word in \tilde{X} and \tilde{Y} .

- **SPL:** the main idea of path-based measures is that the similarity between two concepts is a function of the length of the path linking the concepts and the position of the concepts in the taxonomy. The SPL distance which is a variant of the distance methods of [64], [66] has been widely used to measure the semantic similarities of different concepts in WordNet [59]. As the SPL based on WordNet has shown its talents and attracted great concern, we also use SPL to measure the relevance between two sets of concepts. Depending on the structure of WordNet, generally the result obtained from hypernym relation is regarded as the similarity between concepts. Let us define the length of the shortest path from synset c_i to synset c_j in WordNet as $len(c_i, c_j)$, then $len(c_i, c_j)$ is counted as the actual path length between c_i and c_j . For example, if c_i and c_j are not the same node, but c_i is the parent of c_j , we assign the semantic length between them to 1, i.e., $len(c_i, c_j) = 1$. In this way, for one category c_{xi} in the dataset \mathbb{D}_x , its SPL distance to the dataset \mathbb{D}_y is denoted as $d(c_{xi}, \mathbb{D}_y) = \frac{1}{M} \sum_{j=1}^M len(c_{xi}, c_{yj})$, where M is the number of categories in \mathbb{D}_y . Finally, the SPL distance between \mathbb{D}_x and \mathbb{D}_y is $\mathcal{D}_{spl}(\mathbb{D}_x, \mathbb{D}_y) = \frac{1}{N} \sum_{i=1}^N d(c_{xi}, \mathbb{D}_y)$, where N is the number of categories in \mathbb{D}_x .

For the WMD distance, the results are shown in Table 1. We utilize the approach [61] under the setting where the words are represented with the word2vec [65] embedding vectors. The WMD distance between two categories is a specific case where each set only contains one entity. For example, the WMD distance between the entity “basset” (i.e., n02088238) and the entity “beagle” (i.e., n02088364) which both belong to the DOG branch is 3.0119. The WMD distance between the entity “basset” and the entity “flattop”

(i.e., n02687172) is 4.0327, which is much bigger as the entity "flattop" belongs to the ARIN branch. It is illustrated that "basset" is close to "beagle" while "basset" is far away from "flattop". As these categories are special entities selected from different divided branches of ImageNet, the distance between two sets of categories will be within these ranges. So it can be concluded that the WMD distance between two sets roughly varies from 3 to 5. For a holistic view, the WMD distances among the DOG, LTED, ARIN, and AROT branches are shown in Table 1. The results demonstrate that the categories in the some branch have bigger relevance. As the results show, the WMD distance between DOG and LTED, denoted as $\mathcal{D}_{wmd}(DOG, LTED)$, is 3.1981. However, $\mathcal{D}_{wmd}(DOG, ARIN)$ and $\mathcal{D}_{wmd}(DOG, AROT)$ are 3.5829 and 3.5438 respectively, which are much bigger compared with $\mathcal{D}_{wmd}(DOG, LTED)$. Because DOG and LTED are corresponded to the living thing branch, they are more relevant with each other, compared to ARIN and AROT which are covered by the artifact branch. Meanwhile, $\mathcal{D}_{wmd}(ARIN, AROT)$ is 3.3787, while $\mathcal{D}_{wmd}(ARIN, LTED)$ is 3.5102. Because $\mathcal{D}_{wmd}(ARIN, LTED)$ is much bigger than $\mathcal{D}_{wmd}(ARIN, AROT)$, it is demonstrated that ARIN is more relevant with AROT, rather than LTED.

The results based on the SPL metric are shown in Table 2. The SPL distance between the entity "basset" (i.e., n02088238) and the entity "beagle" (i.e., n02088364) is 2. Note that the entity "hound" (i.e., n02087551) is the parent node of both "basset" and "beagle". The SPL distance between the entity "basset" and the entity "flattop" (i.e., n02687172) is 22, as the entity "flattop" belongs to the ARIN branch. From these cases, it also can be concluded that the SPL distance between two sets roughly varies from 2 to 22. The SPL distances among the DOG, LTED, ARIN, and AROT branches are shown in Table 2. The SPL distance between DOG and LTED, denoted as $\mathcal{D}_{spl}(DOG, LTED)$ is 13.39. However, $\mathcal{D}_{spl}(DOG, ARIN)$ and $\mathcal{D}_{spl}(DOG, AROT)$ are 16.12 and 15.40 respectively, which are much bigger than $\mathcal{D}_{spl}(DOG, LTED)$. Meanwhile, $\mathcal{D}_{spl}(ARIN, AROT)$ is 10.80, while $\mathcal{D}_{spl}(ARIN, LTED)$ and $\mathcal{D}_{spl}(AROT, LTED)$ are 16.12 and 15.40 respectively. Both of them are much bigger than $\mathcal{D}_{spl}(ARIN, AROT)$. The trend is the same with the one under the measure of WMD, as shown in Table 1.

All the results under two metrics illustrate that the datasets covered by the same branch have smaller distances, demonstrating that the categories in the some branch have bigger relevance. Furthermore, the quantitative results are consistent with the qualitative results. WMD measures the relevances among different datasets or branches based on the semantic embedding vectors of the composed entities, while SPL measures the relevance of them depending on how close of the entities are in the taxonomy. They depict the relevance among different datasets complementarily, and they offer and establish baseline distributional metrics for comparing sets of concepts in computer vision tasks.

Base and novel categories are sampled from the LTED, ARIN, and AROT branches to explore the dataset diversity for FSIR. In this section, we do not use the DOG branch since this branch lacks of diversities of images. The few-shot learning model would suffer from handling a sequence

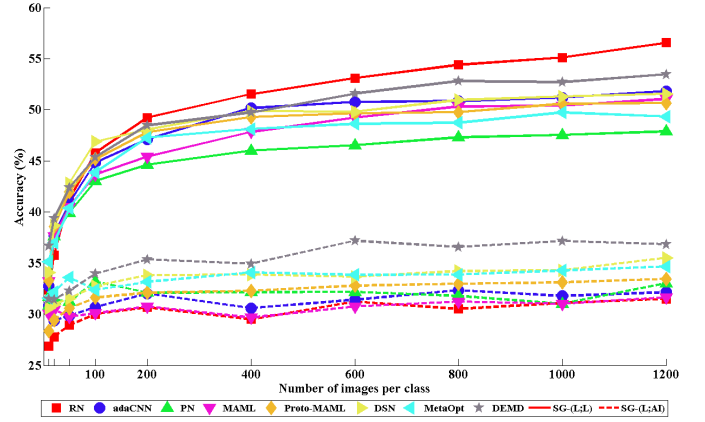


Fig. 4. 5-way 1-shot accuracy of SG-(L;L) and SG-(L;AI).

of training tasks originated from different distributions if the novel categories are irrelevant to the base categories. In the following sub-sections, we carry out various groups of experiments, based on different base and novel categories. A group of experiments includes original or with additional base categories and novel categories, as illustrated in Fig 3. Each group of experiments is conducted 5 times with eight few-shot learning methods (e.g., PN [9], RN [10], DSN [23], DEMD [21], MAML [13], adaCNN [14], Proto-MAML [27], MetaOpt [12]) to obtain stable and reliable performance. The eight methods use a 4 convolutional layers as the meta-learner (backbone) with the different number of filters per layer. We adopt the architectures of corresponding methods without modification for our experiments. Without loss of generality, we analyze the factors of dataset diversity on 1-shot models. To evaluate each model, 400 test tasks are randomly sampled from 20 novel categories. And each test task has 5 classes, each of which has 1 image in the support set and 15 images in the target set. These test settings have been widely used in the few-shot evaluation [9], [10], [13], [14], [22], [26], and the results are reported with mean accuracy.

4.3 Instance Density

This subsection studies the problem of whether increasing the instance density can bring better performance on test tasks. Different from the study of the impact of the shot number [67], this subsection aims to investigate the impact of performance as the number of samples per base category increases. We conduct two groups of experiments with the samples growth (SG) per base category, and each of them uses 64 base categories with the number of samples per category ranging from 10 to 1,200. One group uses base and novel categories sampled from LTED branch, denoted as SG-(L;L). Another group uses the same base categories, but it employs novel categories sampled from ARIN branch, denoted as SG-(L;AI). Each novel category in SG-(L;L) has more relevant base categories than that in SG-(L;AI). In other words, SG-(L;L) uses relevant base categories while SG-(L;AI) employs irrelevant ones.

Fig. 4 displays the performance of two groups. It can be observed that: i) The performance of SG-(L;L) exceeds SG-(L;AI) by a wide margin with the same methods, especially

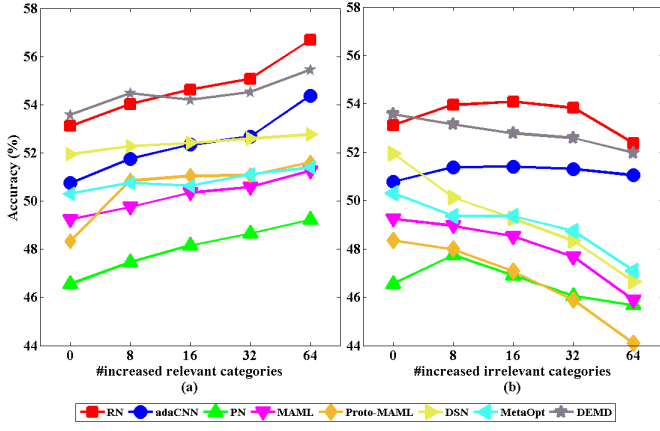


Fig. 5. 5-way 1-shot accuracy of CG-(L,L;L) (a) and CG-(L,AO;L) (b).

as the number of samples per base category increases. ii) In SG-(L;L), more instances lead to better performance, and the performance improvement is fast when the number of samples per base category ranges from 10 to 200, while it gets slow when starting from 200. iii) In SG-(L;AI), the performance is improved at the beginning of the number of instances increasing (from 10 to 100), after which the performance is not significantly improved.

The following suggestions can be obtained.

- It is very important to use plenty of instances from relevant base categories to train the FSIR model.
- If the relevant base categories are not available, there is no need to use too many instances of each category.

4.4 Category Diversity

This subsection studies whether increasing the category diversity can bring better performance on test tasks. Since the number of base categories is changed, we divide base categories into original and additional ones. We set up two groups of experiments with category growth (CG), and each of them uses 64 original base categories and varying additional ones. One group employs original, additional base categories and novel categories all sampled from LTED branch, denoted as CG-(L,L;L). Another group exploits the same original base and novel categories, but it uses additional base categories sampled from AROT branch, denoted as CG-(L,AO;L). It is obvious that CG-(L,L;L) uses relevant additional base categories while CG-(L,AO;L) employs irrelevant ones. The number of samples per original or additional base category is 600. The samples of original base categories are fixed in the same group, and the number of additional base categories ranges from 0 to 64.

Experimental results of CG-(L,L;L) and CG-(L,AO;L) on eight methods are illustrated in Fig. 5 (a) and (b), respectively. It can be observed that: i) When additional base categories are relevant to novel categories, more additional categories lead to better performance (see Fig. 5 (a)). ii) When additional base categories and novel categories are irrelevant, the performance may be improved when the number of categories increases at the beginning, after which the performance drops (see Fig. 5 (b)).

TABLE 3
Sampled categories of different groups.

Groups	Base categories		Novel categories
	Original	Additional	
SG-(L;L)	LTED	-	LTED
SG-(L;AI)	LTED	-	ARIN
CG-(L,L;L)	LTED	LTED	LTED
CG-(L,AO;L)	LTED	AROT	LTED
CG-(L,L;AI)	LTED	LTED	ARIN
CG-(L,AO;AI)	LTED	AROT	ARIN
CGS-(L,L;L)	LTED	LTED	LTED
CGS-(L,L;AI)	LTED	LTED	ARIN
CGS-(L,AO;L)	LTED	AROT	LTED
CGS-(L,AO;AI)	LTED	AROT	ARIN

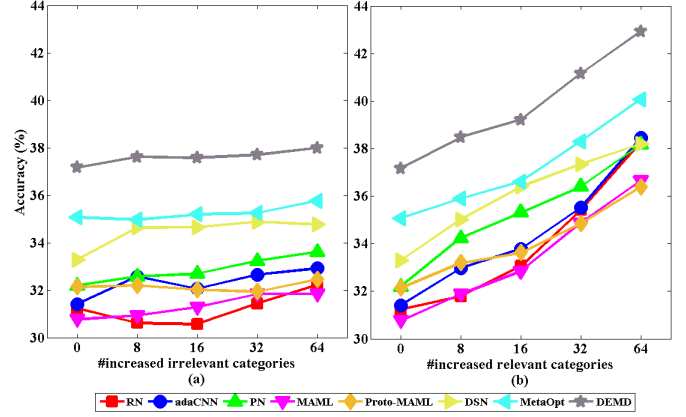


Fig. 6. 5-way 1-shot accuracy of CG-(L,L;AI) (a) and CG-(L,AO;AI) (b).

On the other hand, we set another two groups of experiments denoted as CG-(L,L;AI) and CG-(L,AO;AI). Different from the above two groups, novel categories of them are sampled from ARIN branch, as illustrated in Table 3. Obviously, CG-(L,L;AI) uses irrelevant additional base categories while CG-(L,AO;AI) employs relevant ones.

Experimental results of CG-(L,L;AI) and CG-(L,AO;AI) on eight methods are illustrated in Fig. 6 (a) and (b), respectively. It can be observed that: i) The performance of CG-(L,AO;AI) is obviously superior to CG-(L,L;AI) as the number of additional base categories increases. The main reason is that CG-(L,AO;AI) uses relevant additional base categories while CG-(L,L;AI) uses irrelevant ones. ii) The performance of two groups is improved as the number of additional base categories increases. In addition, comparing CG-(L,L;L) and CG-(L,AO;AI) (or CG-(L,AO;L) and CG-(L,L;AI)), relevant original base categories provide better initial performance than irrelevant ones.

The following suggestions can be obtained.

- It is very important to use plenty of relevant base categories to learn the FSIR model.
- If original base categories are not relevant to novel categories, we can use some additional base categories without constraints.

4.5 Instance Density v.s. Category Diversity

From the above experiments, the FSIR performance would be improved by increasing relevant instances or relevant categories of base categories. To further explore which factor

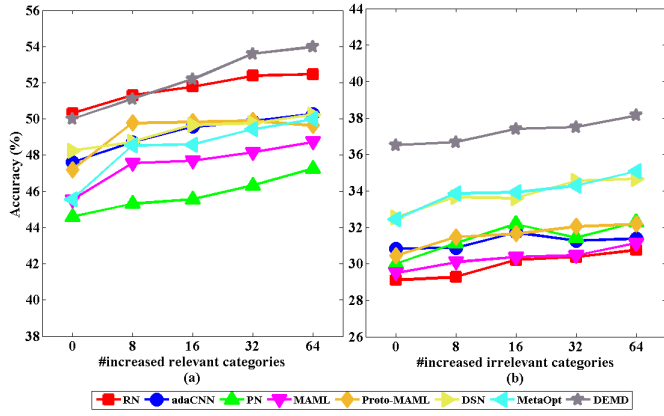


Fig. 7. 5-way 1-shot accuracy of CGS-(L,L;L) (a) and CGS-(L,L;AI) (b).

is more effective to boost the performance, we make comparisons by fixing the number of total samples while varying the number of categories and the number of samples in each category. In this case, the number of samples in each category will be decreased to guarantee the same total number of samples, as the number of base categories increases. Since the relevance of base and novel categories would affect the performance, we set up two groups of experiments with the same relevance of original and additional base categories, and each of them includes 32 original base categories and varying additional ones. One group employs categories all sampled from LTED branch, denoted as CGS-(L,L;L) (Category Growth under the Same total samples). Another group exploits the same original and additional base categories, but it uses novel categories sampled from ARIN branch, denoted as CGS-(L,L;AI). Thus CGS-(L,L;L) uses relevant base categories while CGS-(L,L;AI) employs irrelevant ones. Original base categories are fixed in the same group of experiments, and the number of additional base categories ranges from 0 to 64. The total number of samples of base categories is 38,400 (equal to the number of total training samples in MiniImageNet), where each base category contains equal number of samples. Since the total number of samples of base categories is fixed, each original base category would have less samples with the growth of the number of additional base categories. For example, each original base category contains 1,200 samples without additional base categories (the total number is $1200 \times 32 = 38,400$), and the number of samples of each original base category would reduce to 800 when 16 additional base categories with 800 samples per category are used (the total number is $800 \times (32 + 16) = 38,400$).

Experimental results of CGS-(L,L;L) and CGS-(L,L;AI) on eight methods are illustrated in Fig. 7 (a) and (b), respectively. It can be observed that increasing base categories is more effective than increasing their samples to boost the FSIR performance, when original and additional base categories are relevant. That is to say, it is better for the FSIR model to use more relevant base categories than more samples per relevant base category (obtained from Fig. 7 (a)), and it is better for the FSIR model to use more irrelevant base categories than more samples per irrelevant base category (obtained from Fig. 7 (b)). This phenomenon

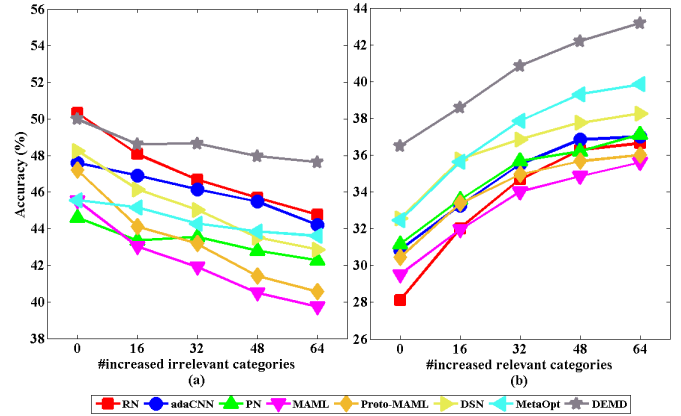


Fig. 8. 5-way 1-shot accuracy of CGS-(L,AO;L) (a) and CGS-(L,AO;AI) (b).

explains that additional base categories provide more bonus for the FSIR model than learned categories with additional samples, since the model has already learned accurate knowledge from hundreds of samples per base category.

Moreover, we set another two groups of experiments with irrelevance of original and additional base categories. The two groups are denoted as CGS-(L,AO;L) and CGS-(L,AO;AI), which are different from the above two groups since they use additional base categories sampled from AROT branch, as illustrated in Table 3. Obviously, CGS-(L,AO;L) uses irrelevant additional base categories while CGS-(L,AO;AI) employs relevant additional ones, and CGS-(L,AO;L) uses relevant original base categories while CGS-(L,AO;AI) employs irrelevant original ones.

Experimental results of CGS-(L,AO;L) and CGS-(L,AO;AI) on eight methods are illustrated in Fig. 8 (a) and (b), respectively. From Fig. 8 (a), it is better for the FSIR model to use more samples per relevant base category than more irrelevant base categories. From Fig. 8 (b), it is better for the FSIR model to use more relevant base categories than more samples per irrelevant base category. These two observations can explain that relevance is a more important factor than more base categories or more sample per base category.

The following suggestions can be obtained.

- It is better for the FSIR model to use more base categories than more samples per category, when original and additional base categories are relevant.
- Relevance is a more important factor than transformations in sample forms (i.e., more categories or more sample per category).

According to the above two points, we can further infer that the FSIR performance goes down in order of more relevant base categories, more samples per relevant base category, more irrelevant base categories, and more samples per irrelevant base category.

4.6 Tremendous Number of Categories

When the number of total base samples is fixed, whether increasing the number of base categories will improve performance? To explore this problem, we conduct experiments

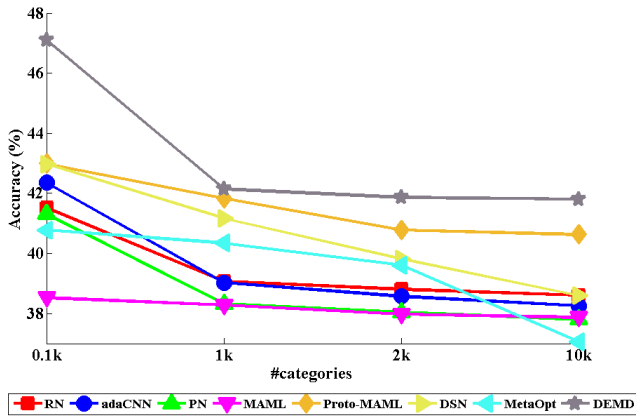


Fig. 9. Experimental results on a large number of categories with a fixed amount of total samples.

on a dataset of a larger number of categories. This dataset contains 10,020 categories, sampled from ImageNet [16]. In this case, we set the total number of samples as 20,000, and the number of base categories ranges from 100 to 10,000. Thus each category contains samples ranging from 200 to 2. For each setting (indexed with the number of base categories), the evaluations are also conducted 5 times with eight few-shot learning methods. For the evaluation of each model, we use the same architecture of few-shot learning methods, the same number of test tasks or novel categories, and evaluation index as the above experiments.

Experimental results on eight methods are illustrated in Fig. 9. With the fixed number of total samples, as the number of base categories increases, the FSIR performance decreases. When the number of per base category is 1,000, namely each base category contains 20 samples, more samples per base category become more important than more base categories. In this case, additional samples per base category provide more bonus for the FSIR model than additional base categories, since the FSIR model can not learn accurate knowledge well from a small amount of samples per category.

4.7 Discussion

The main factors about base categories affecting the performance of FSIR are presented as follows:

- The more categories are not always the better. Relevance is the key factor, and increasing relevant categories can benefit FSIR, otherwise, including irrelevant categories may not be helpful.
- Data diversity is also an important factor to FSIR, and large diversity in categories or density in instances can result in better results, enhancing the generalization capability of the FSIR model.
- When enough instances are in each category, category diversity is more sensitive than instance density, which may coarsely broaden the diversity of the whole dataset.

5 EVALUATION OF DATASET STRUCTURE

In early studies, FSIR methods attempt to recognize the alphabet images [18] or the object images [17] with simple



Fig. 10. Example illustrations of different levels of image complexity.

background. Afterwards, FSIR methods focus on more realistic images, such as general object images [9], [10], [22], [30], fine-grained object images [22], [68], scene images [28], [31]. However, different type of images have intrinsic properties and data structures, which may lead to significant performance differences. In this section, we study the dataset structure through the view of FSIR. First, we present various factors of dataset structures with quantitative representations. Second, we introduce several datasets under few-shot settings. Finally, we make analysis on different datasets from the dataset structure and few-shot learning methods.

5.1 Factors of Dataset Structure

Dataset structure can be reflected with image complexity, intra-concept visual consistency and inter-concept visual similarity. Image complexity can depict visual contents of original images. If original images include complex background information, it could be difficult to accurately identify their concepts. As illustrated in Fig. 10, the apple image is more complex than the letter “L” image, and the scene image with cluster background is more complex than the apple image. Both intra-concept visual consistency and inter-concept visual similarity can depict semantic gaps between low-level visual features (i.e., computational representations of images from hand-crafted algorithms) and high-level image concepts (i.e., semantic interpretations of images from human beings) [69]. Intra-concept visual consistency describes the aggregations of single concept in the visual feature space, and a big intra-concept visual consistency may result in low semantic gaps. In contrast, inter-concept visual similarity describes correlations between different concepts in the visual feature space, and a small inter-concept visual similarity may result in low semantic gaps. When considering intra-concept visual consistency and inter-concept visual similarity simultaneously, we obtain that a larger difference value between them means a smaller semantic gap.

We quantify image complexity with the following ways: i) Complex images often have complex structures, and structural attributes can be preserved by edges. We use percentage of edge points P_{EP} as a metric, defined as:

$$P_{EP} = \frac{\#(\text{edge pixels})}{\#(\text{image pixels})} \quad (6)$$

where $\#(\text{image pixels})$ and $\#(\text{edge pixels})$ are the number of pixels and edges in the image, respectively. Edge pixels can be detected with the Canny edge detection method [70]. ii) We utilize the 2D entropy E_{2D} [71] to measure the underlying spatial structure and pixel co-occurrence. Given an $N \times M$ pixel image $f(n, m)$, E_{2D} is defined as:

$$E_{2D} = - \sum_{i=I_{min}}^{I_{max}} \sum_{j=J_{min}}^{J_{max}} p_{i,j} \log_2 p_{i,j} \quad (7)$$

where $p_{i,j} = \frac{1}{N \times M} \sum_{n=1}^N \sum_{m=1}^M \delta_{i,f_x(n,m)} \delta_{j,f_y(n,m)}$, δ is the Kronecker delta formulation, f_x and f_y are the two derivative components of the gradient field, I and J record all gradient values in two gradient directions.

Intra-concept visual consistency and inter-concept visual similarity are quantified according to [69]. Intra-concept visual consistency of category C_l is defined as: $c_{ina}(C_l) = \frac{2}{|C_l| * (|C_l| - 1)} \sum_{i=1}^{|C_l|} \sum_{j=i+1}^{|C_l|} k(x_i^i, x_l^j)$, where $|C_l|$ is the number of images in C_l , x_l^i and x_l^j are the feature representations of images in C_l . $k(x_l^i, x_l^j) = c / \sqrt{|\frac{x_l^i - u}{\sigma} - \frac{x_l^j - u}{\sigma}|^2 + c}$, where c is a scalar, $k(x_l^i, x_l^j)$ is inversely proportional to the Euclidean distance of $\frac{x_l^i - u}{\sigma}$ and $\frac{x_l^j - u}{\sigma}$ (μ and σ are the mean and standard deviation of all x , $\frac{x_l^i - u}{\sigma}$ can be regarded as Z-score normalization of all x), and can be used as the similarity of them. The overall intra-concept visual consistency C_{ina} of all categories in D is defined as:

$$C_{ina} = \frac{1}{|D|} \sum_{l=1}^{|D|} c_{ina}(C_l) \quad (8)$$

where $|D|$ is the number of categories in D . Inter-concept visual similarity between C_l and C_k is defined as: $s_{inr}(C_l, C_k) = \frac{1}{|C_l| |C_k|} \sum_{i=1}^{|C_l|} \sum_{j=1}^{|C_k|} k(x_l^i, x_k^j)$, where $|C_l|$ and $|C_k|$ are the number of images of C_l and C_k , respectively, x_l^i and x_k^j are the feature representations of images in C_l and C_k . The overall inter-concept visual similarity S_{inr} of each two categories in D is defined as:

$$S_{inr} = \frac{2}{|D|(|D| - 1)} \sum_{l=1}^{|D|} \sum_{k=l+1}^{|D|} s_{inr}(C_l, C_k) \quad (9)$$

We use three types of classical features (i.e., GIST: used in [72], HOG: Histograms of Oriented Gradients [73], LBP: Local Binary Patterns [74].) to calculate C_{ina} and S_{inr} , and set $c = 1.0$. We believe that classical descriptors can somewhat convey the internal structure of datasets from multiple aspects. In addition to the classical descriptors, we also include convolutional neural network (CNN) and bag-of-word (BoW) features for comparison, which may be biased to the training data. In our case CNN model is pretrained on ImageNet, codebook of BoW is learned within each dataset. As illustrated in Table 7, the trends of the statistical results on different datasets are almost the same

TABLE 4
The image complexity in different datasets.

Datasets	P_{EP}	E_{2D}
MiniCharacter	0.048	2.190
MiniImagenet	0.225	7.045
MiniPlaces	0.254	7.411
MiniFlower	0.325	8.012
MiniFood	0.259	7.407

in most cases, making the analysis be more comprehensive. It can be observed that in all cases (using different types of features in different datasets), the intra-concept similarity is larger than inter-concept similarity. HOG and LBP descriptors focus more on local details, which are sensitive to the content of dataset, resulting in larger deviation among different datasets. In contrast, GIST, BoW, and CNN focus more on global information, where more consistent results are obtained in different datasets.

5.2 Datasets and Settings

We construct several datasets with different structures, which range from simple character images to the images with one or more objects. In addition to the above images, facing vertical fields, some fine-grained datasets (i.e., food and flower datasets) are also used in our evaluations. To balance the diversity of different datasets, we refer to Mini-Imagenet, and organize the datasets with the same number of categories and the same number of samplers per category as MiniImagenet. These datasets are collected as follows. i) **MiniCharacter** is handwritten character dataset, which is generated and annotated by 15 volunteers. MiniCharacter includes various characters such as English letters, numbers, mathematical symbols. The total number of categories is 84, and each of category has 100 images. The 64 and 20 categories are used as base and novel categories, respectively. ii) **MiniImagenet** [22] uses 64 and 20 categories as base and novel categories, respectively, where each category contains 600 images. iii) **MiniPlaces** is a subset of Places365 [6]. It uses 64 and 20 categories as base and novel categories, respectively, where each category contains 600 images. iv) **MiniFlower** is sampled from flower dataset [75] provided from 2018 FGCVxFlower Classification Challenge. It uses 64, 20 categories as base, novel categories, respectively, where each category contains 600 images. v) **MiniFood** is sampled from Food101 [76]. It uses 64 and 20 categories as base and novel categories, respectively, where each category contains 600 images. Experiments are conducted with eight few-shot learning methods (i.e., PN, RN, DSN, DEMD, MAML, adaCNN, Proto-MAML, MetaOpt). Evaluating each model, we use the same number of test tasks, evaluation index and the same architecture of few-shot learning methods (denoted as CNN-4), as Sect. 4. Besides, we also use a deeper architecture ResNet-12, which has been widely adopted in recent works [12], [14], [21], [23], [77].

5.3 Analysis on Dataset Structure

Our goal is to analyze the performance of different dataset from their structures. Table 4 illustrates the image complexity of different datasets. which is measured with P_{EP}

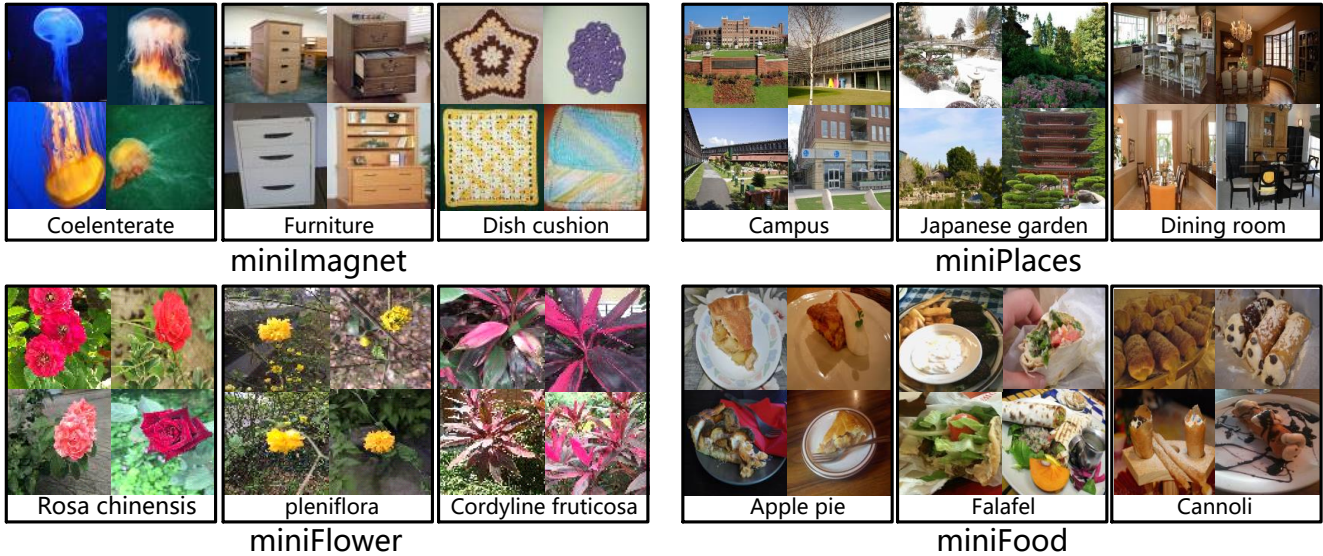


Fig. 11. Some image examples in different datasets.

TABLE 5
5-way 1-shot accuracy (%) on different datasets with CNN-4.

Datasets	Metric-based methods				Meta-learning methods			
	PN	RN	DSN	DEMD	MAML	adaCNN	Proto-MAML	MetaOpt
MiniCharacter	86.17	91.83	87.21	88.43	85.45	83.91	88.00	88.80
MiniImagenet	49.42	51.38	51.03	52.46	48.70	48.26	48.41	51.67
MiniPlaces	49.00	50.62	51.89	53.96	48.49	50.05	50.44	55.74
MiniFlower	48.73	50.73	51.07	55.24	49.32	48.56	50.60	51.95
MiniFood	41.41	45.68	44.86	50.70	43.55	44.94	43.63	45.73

TABLE 6
5-way 1-shot accuracy (%) on different datasets with ResNet-12.

Datasets	Metric-based methods				Meta-learning methods			
	PN	RN	DSN	DEMD	MAML	adaCNN	Proto-MAML	MetaOpt
MiniCharacter	92.87	92.15	92.70	93.49	85.65	89.26	94.24	93.10
MiniImagenet	58.47	53.08	58.67	60.46	54.90	57.13	57.37	59.73
MiniPlaces	60.55	58.01	61.30	60.47	58.25	56.35	60.4	63.12
MiniFlower	55.63	55.36	55.26	61.62	54.15	58.10	55.13	58.53
MiniFood	51.35	49.29	51.58	54.76	49.44	52.15	50.63	52.30

and E_{2D} . Table 5 and Table 6 show the results of different methods on different datasets. It can be observed that the image complexity in MiniCharacter is the lowest. Each character image contains only one character with clear background. Table 5 also demonstrates that the performance on MiniCharacter is significantly higher than the one on the other datasets. From this special case of MiniCharacter, we can find that image complexity plays an important role in FSIR, where lower complexity often leads to higher performance. However, character images are very different with most real-world images, such as object, scene and food images. In the rest evaluations, we mainly focus on comparisons and discussions of the other four datasets.

As illustrated in Table 4, MiniFlower is the highest in image complexity. However, the FSIR performance on MiniFlower is not the lowest (see Table 5 and Table 6), which is higher than MiniFood and comparable with MiniImagenet. This may be explained from the following reasons: i) MiniFlower is a special kind of fine-grained image dataset, where images in the same category are very similar. As

shown in Fig. 11, although image complexity is very high in the aspects of clustered edges and detailed component information, the visual texture and structural patterns of images in the same category are still very similar. MiniFlower has the highest intra-concept visual consistency C_{intra} , as illustrated in Table 7. This may present that the task of flower recognition is relatively easier, even for the case of FSIR. ii) As categories in MiniFlower all belong to flower and they are biological relatives, it is intuitive that visual patterns of different flower categories are also similar to some extent, as shown in Fig. 11. Thus base categories and novel categories in miniFlower present some relevance, which enables learned FSIR models to better recognize novel categories.

Except for the very simple dataset MiniCharacter, most methods obtain the highest performance on MiniPlaces (see Table 5 and Table 6). MiniFlower is more complex than MiniPlaces (see Table 4), which seems to be the reason that most methods obtain lower performances on MiniFlower than that on MiniPlaces. MiniPlaces has comparable image

complexity to the MiniFood, however, the average gains of all methods on MiniPlaces (over MiniFood) are close to 6.8% in Table 5 and 7.8% in Table 6. In alternative to the absolute complexity, such difference in accuracy may be caused by the difference value between intra-concept visual consistency and inter-concept visual similarity with CNN features in Table 7, where MiniPlaces dataset has a larger difference value. Similarly, MiniImagenet has a smaller difference value than MiniPlaces, thus, most methods still obtain higher performances on MiniPlaces compared to MiniImagenet.

The FSIR performance on MiniImagenet is higher than MiniFood and comparable with MiniFlower. The main reason is that image complexity in MiniImagenet is lower than the one in the two datasets. However, the advantage of performance on MiniImagenet is faint or not obvious when considering its image complexity is obviously lower than that of MiniFlower. This phenomenon can be attributed to less relevance of base categories and novel categories in MiniImagenet, which is reflected in the following two aspects. i) Category labels in MiniImageNet are sampled from a larger semantic space which brings greater diversities of semantic concepts, compared with MiniFlower. This leads to less probabilities of sampling relevant base and novel categories in MiniImagenet, when the number of base categories or novel categories are the same in all datasets (i.e., all datasets include 64 base categories and 20 novel categories). ii) Images in MiniImagenet focus on single object, and different categories differ greatly in visual content, in contrast, different categories in MiniFlower are similar, as shown in Fig. 11. Thus base categories and novel categories in MiniImagenet present less relevance than that in MiniFlower.

The FSIR performance from all methods on MiniFood is the worst. The reasons can be explained as follows. i) As shown in Table 4, the image complexity of MiniFood is much higher than the one of MiniImagenet and comparable with MiniPlaces. Besides, compared with the two datasets, the inter-concept visual similarity S_{inr} of MiniFood is higher (see Table 7). Therefore, the performance on MiniFood is worse than the one on MiniImagenet and MiniPlaces. ii) Although MiniFlower and MiniFood both belong to fine-grained datasets, there are fixed semantic patterns in MiniFlower. For example, the flower consists of some semantic parts, such as petals and calyx. However, such semantic patterns do not exist in minFood [78], and minFood thus has a lower intra-concept visual consistency C_{ina} than MiniFlower (see Table 7). Therefore, the FSIR performance on MiniFood is worse than the one on MiniFlower.

5.4 Analysis on Few-shot Learning Methods

As shown in Fig. 12 (a), for all methods, with a deeper backbone ResNet-12, PN obtains the largest performance gain averaged on the five datasets (8.83%). The probable reason is that a deeper network makes PN learn better prototypical representation compared with shallow networks. In contrast, the averaged gain from all datasets is the lowest (3.53%) for RN. RN can obtain powerful features from the deep backbone ResNet-12. In this case, a simple metric is enough for effective few-shot learning. However, RN

adopts a more complex metric implemented by convolutional transformation, leading to the limited generalization ability. Both PN and RN belong to metric-based methods, while among different meta-learning methods, MAML obtains the smallest averaged gain from the backbone of CNN-4 to ResNet-12. Compared to adaCNN and MetaOpt, MAML needs to learn the same initialization, from which different tasks can achieve effective adaptation with gradient descent. However, compared to the shallow backbone (CNN-4), it's more difficult to obtain better initialization on the deeper backbone (ResNet-12), due to the larger parameter space for initialization. In contrast, Proto-MAML initializes the classifier with the class prototype, achieving a good initialization when using the backbone ResNet-12. Thus the gain of Proto-MAML is much higher than MAML, and comparable to adaCNN and MetaOpt. As shown in Fig. 12 (b), All methods obtain the performance gain from one shallow backbone (CNN-4) to a deeper backbone (ResNet-12). Particularly, the average gain of all methods on MiniCharacter is the smallest (4.21%), which is intuitive, as images in MiniCharacter is very simple. The average gain on MiniPlaces is the biggest (8.53%). The reason is that images in MiniPlaces usually contain multiple objects, using deeper architectures with more convolutional and pooling operations can progressively generate more abstract feature representations for this kind of images.

In metric-base methods, DSN and DEMD outperform classical metric-based methods PN and RN, benefiting from the more effective metric learning methods. In particular, DSN learns task-adaptive different subspace metrics, and DEMD uses the Earth Mover's Distance to capture detailed differences of each two images in local regions. And compared with other meta-learning methods, such as adaCNN, MAML and Proto-MAML, MetaOpt obtains better accuracy on most datasets (except for miniCharacter). In particular, MetaOpt can share common parameters (in backbone models) for different tasks, allowing to focus on the optimizing of high-level classifiers, leading to fast adaptation with only few shots in training. Among metric-based/meta-learning methods, DEMD/MetaOpt obtains better results on most datasets. When comparing with best meta-learning (MetaOpt) and metric-based (DEMD) methods, the former works better on datasets with more objects in larger difference value between intra-concept consistency and inter-concept similarity, such as MiniPlaces, while the latter works better on more fine-grained datasets, such as MiniFlower and MiniFood. DEMD and MetaOpt obtain comparable results on more simple datasets with smaller complexity (in Table 7), such as MiniCharacter and MiniImageNet. Since miniPlaces dataset usually consists of object co-occurrences between different categories, sharing the common parameters and focusing on high-level discrimination allow MetaOpt to obtain better performance on miniPlaces. Since different categories in fine-grained datasets usually contain similar prototypes, DEMD can focus more on detailed regions, leading to better performance on more fine-grained datasets.

One interesting method is Proto-MAML, a meta-learning method like MAML, whose classifier is initialized with the class prototype from metric-based method PN. Thus, the comparison between ProtoMAML, MAML and PN is worth

TABLE 7
Intra-concept visual consistency and inter-concept visual similarity in different datasets.

Datasets	C_{ina} (%)					S_{inr} (%)				
	GIST	BoW	CNN	HOG	LBP	GIST	BoW	CNN	HOG	LBP
MiniImagenet	0.45	2.40	5.11	0.25	11.24	0.37(0.08)	2.23(0.17)	4.90(0.21)	0.20(0.05)	7.64(3.60)
MiniPlaces	0.44	2.40	4.96	0.27	4.22	0.36(0.08)	2.23(0.17)	4.73(0.23)	0.20(0.07)	3.63(0.59)
MiniFlower	0.55	2.38	5.29	0.44	18.91	0.46(0.09)	2.22(0.16)	5.11(0.18)	0.37(0.07)	17.74(1.17)
MiniFood	0.45	2.40	5.16	0.31	11.67	0.39(0.06)	2.23(0.07)	4.97(0.19)	0.25(0.06)	11.24(0.43)

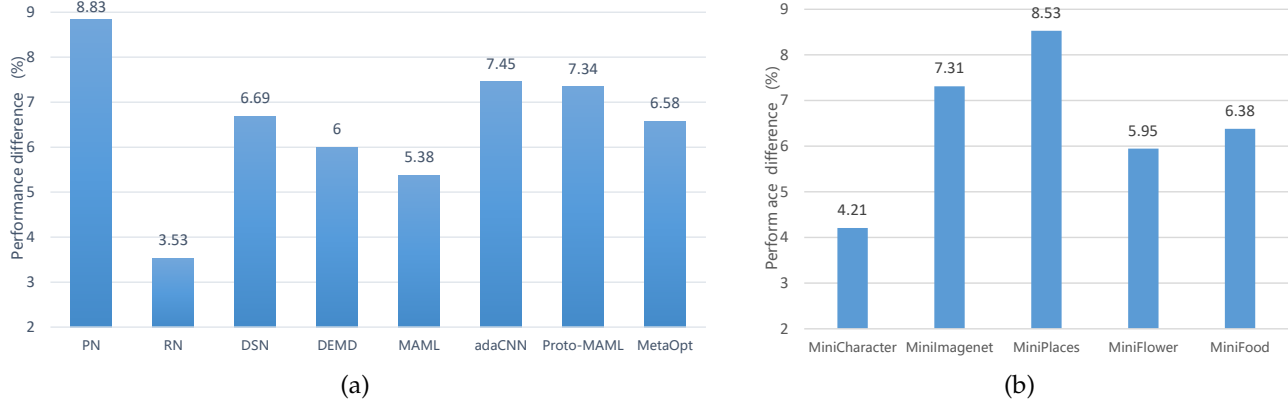


Fig. 12. (a): the average gain from CNN-4 to ResNet-12 over all datasets for different methods. (b): the average gain from CNN-4 to ResNet-12 over all methods on different datasets.

discussing. The results of Proto-MAML on MiniImagenet is in line with the reported results in [27], where the accuracy of Proto-MAML is slightly worse than PN. However, compared with MAML and PN, Proto-MAML obtains better performance on three datasets (i.e., MiniCharacter, MiniPlaces, and MiniFood) with CNN-4, and on MiniCharacter with ResNet-12. With a shallow backbone (CNN-4), Proto-MAML works better than PN and MAML on most datasets, demonstrating that a suitable initialization (with PN in Proto-MAML) is also necessary to MAML. Otherwise, the trained model may fall into some suboptimal states due to fast convergence in the shallow architecture. In contrast, with a deeper backbone (ResNet-12), PN works slightly better than Proto-MAML on most datasets, showing that PN can be better optimized with a deeper architecture. Furthermore, when using ResNet-12, MAML obtains a lower performance than PN on all datasets. That’s probably because it is difficult for MAML to learn a good initialization in a large parameter space. Compared to MAML, Proto-MAML can be optimized with better initialization, allowing it to obtain more gains on most datasets.

5.5 Discussion

Based on the above analysis, we can obtain:

- A dataset with a low image complexity presents better performance. Besides, intra-concept visual consistency and inter-concept visual similarity also can influence performance differences.
- Different methods have diverse performance on different types of datasets, which is relevant to two important dimensions, namely dataset structures and the method ability. According to our experimental analysis, the best metric-based method and the best meta-learning one obtain comparable performance

on different datasets. A better metric function is important for metric-based methods while better adaptive strategies are vital for meta-learning methods. Combining better metric function learning with better adaptive strategies can be explored in FSIR.

- It’s more effective to design FSIR architectures according to the characteristics of data distribution. For instance, DEMD focuses more on detailed regions, resulting in better performance on fine-grained datasets. MetaOpt shares common parameters and focuses on optimizing category sensitive classifiers, obtaining best accuracy on miniPlaces with object co-occurrences between different scenes.

6 PERSPECTIVES AND FUTURE DIRECTIONS

According to existing FSIR researches and our observations, we give some prospective analysis on future works from the following aspects.

Transferable FSIR. It is common to utilize prior representations obtained in models which are trained with large examples [79] for new tasks. Our work has demonstrated that the relevance between images in base and novel categories, and the data structures of the images have much influence on the FSIR performance. The results provide criterion for selecting or integrating features for FSIR. Furthermore, there are situations that images in base categories and novel categories have different data distributions [11], [55]. Sometimes, images in novel categories are even coupled with unlabeled data [80]. It is important for few-shot learning methods to eliminate the domain gap between base and novel categories, thus these methods can obtain representations with better generalization ability. The analysis of the dataset bias somewhat reveals the shared information among different examples. These results also provide useful

guidance for designing transductive FSIR models to further improve FSIR performance. Moreover, in real world FSIR scenarios, how to explore knowledge from available images to recognize images in some specific target domains is in high demand. For example, recognizing fine-grained novel categories [81], [82] uses generic base categories instead of fine-grained ones, considering the data from general images is easier to access. Our work has investigated the transferable capability impacted by the dataset bias, introducing insightful observations to effectively obtain adapted representations for FSIR.

Incremental learning of few shot learning. In many applications, it is often desirable to have the flexibility of learning novel concepts, with limited data and without re-training on the full training set, namely Incremental Few-Shot Learning (IFSL) [83], [84], [85], [86]. In this task, the novel classes with only a few labeled examples for each class should be considered based on the trained model for a set of base classes. Similar to existing few-shot learning methods, IFSL should also consider the recognition performance on unseen novel classes. Therefore, some observations from our work can still provide guidance in designing IFSL. For example, if the unseen novel classes are very relevant to based categories, IFSLs can obtain better recognition performance. On the other hand, different from existing few-shot learning methods, IFSL should also consider the recognition performance on base classes. For that, incremental learning is incorporated into the few-shot learning framework. The performance differences on different datasets from dataset structures and different few-shot learning methods are worth exploration. For example, what types of few-shot learning methods lead to better performance of IFSL when combined with incremental learning? Our experimental design and analysis can provide the reference for supporting such exploration. For example, integrating metric-based methods and meta-learning ones based on their different learning mechanisms is worthy of further study.

FSIR on data of non-uniform distributions. Data in non-uniform distribution, such as data in long-tailed distribution (LTD) and out-of-distribution (OOD), is typically challenging to the machine learning models. The vast majority of existing FSIR works assume training data of each base category is even. However, this is a highly restrictive setting, LTD is the most common in real-world scenarios, where some categories have plenty of samples while more categories have only a few ones. One goal of few-shot learning is to address the problem in the recognition with LTD data. Particularly in our work, we demonstrate that larger data (without increasing categories) and diverse category distribution may enhance the generative ability of the model. In addition to long-tailed data distribution, a more challenging task is to deal with the OOD data, where test data is not in the same distribution as training data. How to use this kind of data of non-uniform distributions for FSIR is worth exploring. In our case, we demonstrate that different datasets have various complexity, intra-concept consistency and inter-concept similarity, thus, different datasets are OOD to each other. Mixing those OOD data may damage transferability of the FSIR model, thus, how to filter those noise from the data with mixed distributions is worth researching. Moreover, it's more practical and challenging

to use unlabeled OOD data for data augmentation, thus, few-shot learning with semi-supervised training is also a significant research direction in future.

FSIR with extra knowledge. Since visual data contains complex structural information, it is difficult to directly extract effective knowledge, especially for the generic knowledge which can be used to establish some connections on novel categories. However, this generic knowledge can be relatively easily obtained from some prior knowledge such as attributes [28], [87], word embeddings (learned from large-scale text corpora) [88], [89], [90], relationships of entities [89], [90], [91], knowledge graph [89], [90] etc. This kind of information are complementary for FSIR, and the problem of dataset bias can be alleviated to some extent by applying techniques of information fusion or knowledge transfer. Extra knowledge is useful both for the cases of category diversity or dataset from different domains. As human can easily correlate various kinds of extra knowledge to recognize a new object, we believe FSIR with extra knowledge is a potentially important research topic to improve performance of existing few shot benchmarks as well as for practical applications.

7 CONCLUSIONS

Few-shot image recognition (FSIR) is an important research problem in the machine learning and computer vision community. In this paper, we study FSIR with dataset bias systematically. First, we investigate impact of transferable capabilities learned from distributions of base categories. We introduce instance density and category diversity to depict distributions of base categories, and relevance to measure relationships between base categories and novel categories. Experimental results on different sub-datasets of ImageNet demonstrate the relevance, instance density and category diversity can depict the transferable bias from base categories. Second, we investigate differences in performance on different datasets from characteristics of dataset structures and different few-shot learning methods. We introduce image complexity, intra-concept visual consistency, and inter-concept visual similarity to quantify characteristics of dataset structures. From comprehensive experimental evaluations on five datasets with eight few-shot learning methods, some insightful observations are obtained from the perspective of both dataset structures and few-shot learning methods. We hope these observations are helpful to guide future FSIR research.

REFERENCES

- [1] K. He, X. Zhang, S. Ren, and J. Sun, "Deep residual learning for image recognition," in *Computer Vision and Pattern Recognition*, 2016, pp. 770–778.
- [2] C. Szegedy, S. Ioffe, V. Vanhoucke, and A. A. Alemi, "Inception-v4, inception-resnet and the impact of residual connections on learning," in *Association for the Advancement of Artificial Intelligence*, 2017, pp. 4278–4284.
- [3] G. Huang, Z. Liu, L. van der Maaten, and K. Q. Weinberger, "Densely connected convolutional networks," in *Computer Vision and Pattern Recognition*, 2017, pp. 2261–2269.
- [4] Y. LeCun, Y. Bengio, and G. Hinton, "Deep learning," *Nature*, vol. 521, no. 7553, pp. 436–444, 2015.
- [5] J. Deng, W. Dong, R. Socher, L.-J. Li, K. Li, and L. Fei-Fei, "Imagenet: A large-scale hierarchical image database," in *Computer Vision and Pattern Recognition*, 2009, pp. 248–255.

- [6] B. Zhou, A. Lapedriza, A. Khosla, A. Oliva, and A. Torralba, "Places: A 10 million image database for scene recognition," *IEEE Transactions on Pattern Analysis and Machine Intelligence*, vol. 40, no. 6, pp. 1452–1464, 2018.
- [7] S. Thrun and L. Pratt, "Learning to learn: introduction and overview," *Learning to learn*, pp. 3–17, 1998.
- [8] H. F. Harlow, "The formation of learning sets," *Psychological Review*, vol. 56, no. 1, pp. 51–65, 1949.
- [9] J. Snell, K. Swersky, and R. Zemel, "Prototypical networks for few-shot learning," in *Neural Information Processing Systems*, 2017, pp. 4080–4090.
- [10] F. Sung, Y. Yang, L. Zhang, T. Xiang, P. H. Torr, and T. M. Hospedales, "Learning to compare: Relation network for few-shot learning," in *Computer Vision and Pattern Recognition*, 2018, pp. 1199–1208.
- [11] W.-Y. Chen, Y.-C. Liu, Z. Kira, Y.-C. F. Wang, and J.-B. Huang, "A closer look at few-shot classification," in *International Conference on Learning Representations*, 2019.
- [12] K. Lee, S. Maji, A. Ravichandran, and S. Soatto, "Meta-learning with differentiable convex optimization," in *Computer Vision and Pattern Recognition*, 2019, pp. 10 657–10 665.
- [13] C. Finn, P. Abbeel, and S. Levine, "Model-agnostic meta-learning for fast adaptation of deep networks," in *International Conference on Machine Learning*, 2017, pp. 1126–1135.
- [14] T. Munkhdalai, X. Yuan, S. Mehri, and A. Trischler, "Rapid adaptation with conditionally shifted neurons," in *International Conference on Machine Learning*, 2018, pp. 3661–3670.
- [15] G. S. Dhillon, P. Chaudhari, A. Ravichandran, and S. Soatto, "A baseline for few-shot image classification," in *International Conference on Learning Representations*, 2020.
- [16] O. Russakovsky, J. Deng, H. Su, J. Krause, S. Satheesh, S. Ma, Z. Huang, A. Karpathy, A. Khosla, M. Bernstein *et al.*, "Imagenet large scale visual recognition challenge," *International journal of computer vision*, vol. 115, no. 3, pp. 211–252, 2015.
- [17] L. Fei-Fei, R. Fergus, and P. Perona, "One-shot learning of object categories," *IEEE Transactions on Pattern Analysis and Machine Intelligence*, vol. 28, no. 4, pp. 594–611, 2006.
- [18] B. M. Lake, R. Salakhutdinov, and J. B. Tenenbaum, "Human-level concept learning through probabilistic program induction," *Science*, vol. 350, no. 6266, pp. 1332–1338, 2015.
- [19] A. Santoro, S. Bartunov, M. Botvinick, D. Wierstra, and T. Lillicrap, "Meta-learning with memory-augmented neural networks," in *International Conference on Machine Learning*, 2016, pp. 1842–1850.
- [20] G. Koch, R. Zemel, and R. Salakhutdinov, "Siamese neural networks for one-shot image recognition," in *ICML Deep Learning Workshop*, vol. 2, 2015.
- [21] C. Zhang, Y. Cai, G. Lin, and C. Shen, "Deepemd: Few-shot image classification with differentiable earth mover's distance and structured classifiers," in *Computer Vision and Pattern Recognition*, 2020, pp. 12 203–12 213.
- [22] O. Vinyals, C. Blundell, T. Lillicrap, D. Wierstra *et al.*, "Matching networks for one shot learning," in *Neural Information Processing Systems*, 2016, pp. 3630–3638.
- [23] C. Simon, P. Koniusz, R. Nock, and M. Harandi, "Adaptive subspaces for few-shot learning," in *Computer Vision and Pattern Recognition*, 2020, pp. 4136–4145.
- [24] J. Schmidhuber, "Evolutionary principles in self-referential learning, or on learning how to learn: the meta-meta-... hook," Ph.D. dissertation, Technische Universität München, 1987.
- [25] D. Naik and R. Mammone, "Meta-neural networks that learn by learning," in *International Joint Conference on Neural Networks*, vol. 1, 1992, pp. 437–442.
- [26] T. Munkhdalai and H. Yu, "Meta networks," in *International Conference on Machine Learning*, 2017, pp. 2554–2563.
- [27] E. Triantafillou, T. Zhu, V. Dumoulin, P. Lamblin, U. Evci, K. X. ad Ross Goroshin, K. S. Charles Gelad and, P.-A. Manzagol, and H. Larochelle, "Meta-dataset: A dataset of datasets for learning to learn from few examples," in *International Conference on Learning Representations*, 2020.
- [28] M. Dixit, R. Kwitt, M. Niethammer, and N. Vasconcelos, "Aga: Attribute-guided augmentation," in *Computer Vision and Pattern Recognition*, 2017, pp. 3328–3336.
- [29] Z. Chen, Y. Fu, Y. Zhang, Y.-G. Jiang, X. Xue, and L. Sigal, "Semantic feature augmentation in few-shot learning," *arXiv preprint arXiv:1804.05298*, 2018.
- [30] B. Hariharan and R. Girshick, "Low-shot visual recognition by shrinking and hallucinating features," in *International Conference on Computer Vision*, 2017, pp. 3018–3027.
- [31] E. Schwartz, L. Karlinsky, J. Shtok, S. Harary, M. Marder, A. Kumar, R. Feris, R. Giryes, and A. Bronstein, "Delta-encoder: an effective sample synthesis method for few-shot object recognition," in *Neural Information Processing Systems*, 2018, pp. 2850–2860.
- [32] S. Gidaris, A. Bursuc, N. Komodakis, P. P. Perez, and M. Cord, "Boosting few-shot visual learning with self-supervision," in *International Conference on Computer Vision*, 2019, pp. 8058–8067.
- [33] X. Li, Q. Sun, Y. Liu, Q. Zhou, S. Zheng, T.-S. Chua, and B. Schiele, "Learning to self-train for semi-supervised few-shot classification," in *Neural Information Processing Systems*, 2019, pp. 10 276–10 286.
- [34] M. Ren, S. Ravi, E. Triantafillou, J. Snell, K. Swersky, J. B. Tenenbaum, H. Larochelle, and R. S. Zemel, "Meta-learning for semi-supervised few-shot classification," in *International Conference on Learning Representations*, 2018.
- [35] Y. Liu, J. Lee, M. Park, S. Kim, E. Yang, S. J. Hwang, and Y. Yang, "Learning to propagate labels: Transductive propagation network for few-shot learning," in *International Conference on Learning Representations*, 2019.
- [36] Z. Yu, L. Chen, Z. Cheng, and J. Luo, "Transmatch: A transfer-learning scheme for semi-supervised few-shot learning," in *Computer Vision and Pattern Recognition*, 2020, pp. 12 856–12 864.
- [37] O. Sbai, C. Couprie, and M. Aubry, "Impact of base dataset design on few-shot image classification," *arXiv preprint arXiv:2007.08872*, 2020.
- [38] G. French, M. Mackiewicz, and M. Fisher, "Self-ensembling for visual domain adaptation," in *International Conference on Learning Representations*, 2018.
- [39] W. Zellinger, T. Grubinger, E. Lughofer, T. Natschläger, and S. Saminger-Platz, "Central moment discrepancy (cmd) for domain-invariant representation learning," in *International Conference on Learning Representations*, 2017.
- [40] Y. Ganin and V. Lempitsky, "Unsupervised domain adaptation by backpropagation," in *International Conference on Machine Learning*, 2015, pp. 1180–1189.
- [41] M. Long, Y. Cao, J. Wang, and M. I. Jordan, "Learning transferable features with deep adaptation networks," in *International Conference on Machine Learning*, 2015, pp. 97–105.
- [42] X. Li, L. Herranz, and S. Jiang, "Multifaceted analysis of fine-tuning in deep model for visual recognition," *arXiv preprint arXiv:1907.05099*, 2019.
- [43] H. Azizpour, A. S. Razavian, J. Sullivan, A. Maki, and S. Carlsson, "Factors of transferability for a generic convnet representation," *IEEE Transactions on Pattern Analysis and Machine Intelligence*, vol. 38, no. 9, pp. 1790–1802, 2016.
- [44] M. Long, H. Zhu, J. Wang, and M. I. Jordan, "Unsupervised domain adaptation with residual transfer networks," in *Neural Information Processing Systems*, 2016, pp. 136–144.
- [45] E. Tzeng, J. Hoffman, K. Saenko, and T. Darrell, "Adversarial discriminative domain adaptation," in *Computer Vision and Pattern Recognition*, 2017, pp. 2962–2971.
- [46] J.-Y. Zhu, T. Park, P. Isola, and A. A. Efros, "Unpaired image-to-image translation using cycle-consistent adversarial networks," in *International Conference on Computer Vision*, 2017, pp. 2223–2232.
- [47] J. Hoffman, E. Tzeng, T. Park, J.-Y. Zhu, P. Isola, K. Saenko, A. A. Efros, and T. Darrell, "Cycada: Cycle-consistent adversarial domain adaptation," in *International Conference on Machine Learning*, 2018, pp. 1989–1998.
- [48] Y. Zhang, H. Tang, K. Jia, and M. Tan, "Domain-symmetric networks for adversarial domain adaptation," in *Computer Vision and Pattern Recognition*, 2019, pp. 5031–5040.
- [49] S. Cui, S. Wang, J. Zhuo, C. Su, Q. Huang, and Q. Tian, "Gradually vanishing bridge for adversarial domain adaptation," in *Computer Vision and Pattern Recognition*, 2020, pp. 12 455–12 464.
- [50] M. Mancini, S. R. Bulo, B. Caputo, and E. Ricci, "Adagraph: Unifying predictive and continuous domain adaptation through graphs," in *Computer Vision and Pattern Recognition*, 2019, pp. 6561–6570.
- [51] S. Motiian, Q. Jones, S. M. Iranmanesh, and G. Doretto, "Few-shot adversarial domain adaptation," in *Neural Information Processing Systems*, 2017, pp. 6670–6680.
- [52] B. Kang and J. Feng, "Transferable meta learning across domains," in *Uncertainty in Artificial Intelligence*, 2018, pp. 177–187.

- [53] P. Welinder, S. Branson, T. Mita, C. Wah, F. Schroff, S. Belongie, and P. Perona, "Caltech-ucsd birds 200," 2010.
- [54] H.-Y. Tseng, H.-Y. Lee, J.-B. Huang, and M.-H. Yang, "Cross-domain few-shot classification via learned feature-wise transformation," in *International Conference on Learning Representations*, 2020.
- [55] Y. Guo, N. C. F. Codella, L. Karlinsky, J. R. Smith, T. Rosing, and R. Feris, "A new benchmark for evaluation of cross-domain few-shot learning," *arXiv preprint arXiv:1912.07200*, 2019.
- [56] R. Vuorio, S.-H. Sun, H. Hu, and J. J. Lim, "Multimodal model-agnostic meta-learning via task-aware modulation," in *Neural Information Processing Systems*, 2019, pp. 1–12.
- [57] H. Yao, Y. Wei, J. Huang, and Z. Li, "Hierarchically structured meta-learning," in *International Conference on Machine Learning*, 2019, pp. 7045–7054.
- [58] S. Thrun and L. Pratt, *Learning to learn*. Springer Science & Business Media, 2012.
- [59] G. A. Miller, "Wordnet: a lexical database for english," *Communications of the ACM*, vol. 38, no. 11, pp. 39–41, 1995.
- [60] J. Yosinski, J. Clune, Y. Bengio, and H. Lipson, "How transferable are features in deep neural networks?" in *Neural Information Processing Systems*, 2014, pp. 3320–3328.
- [61] M. J. Kusner, Y. Sun, N. I. Kolkun, and K. Q. Weinberger, "From word embeddings to document distances," in *International Conference on Machine Learning*, 2015.
- [62] L. Chen, Z. Gan, Y. Cheng, L. Li, L. Carin, and J. Liu, "Graph optimal transport for cross-domain alignment," in *International Conference on Machine Learning*, 2020, pp. 1542–1553.
- [63] A. Kutuzov, M. Dorgham, O. Oliynyk, C. Biemann, and A. Panchenko, "Making fast graph-based algorithms with graph metric embeddings," *arXiv preprint arXiv:1906.07040*, 2019.
- [64] R. Rada, H. Mili, E. Bicknell, and M. Blettner, "Development and application of a metric on semantic nets," *IEEE transactions on systems, man, and cybernetics*, vol. 19, no. 1, pp. 17–30, 1989.
- [65] T. Mikolov, I. Sutskever, K. Chen, G. Corrado, and J. Dean, "Distributed representations of words and phrases and their compositionality," *arXiv preprint arXiv:1310.4546*, 2013.
- [66] H. Bulskov, R. Knappe, and T. Andreasen, "On measuring similarity for conceptual querying, Inai 2522," in *Flexible Query Answering Systems 5th International Conference, FQAS*, 2002, pp. 27–29.
- [67] T. Cao, M. T. Law, and S. Fidler, "A theoretical analysis of the number of shots in few-shot learning," in *International Conference on Learning Representations*, 2020.
- [68] X.-S. Wei, P. Wang, L. Liu, C. Shen, and J. Wu, "Piecewise classifier mappings: Learning fine-grained learners for novel categories with few examples," *IEEE Transactions on Image Processing*, vol. 28, no. 12, pp. 6116–6125, 2019.
- [69] J. Fan, X. He, N. Zhou, J. Peng, and R. Jain, "Quantitative characterization of semantic gaps for learning complexity estimation and inference model selection," *IEEE Transactions on Multimedia*, vol. 14, no. 5, pp. 1414–1428, 2012.
- [70] J. Canny, "A computational approach to edge detection," *IEEE Transactions on Pattern Analysis and Machine Intelligence*, no. 6, pp. 679–698, 1986.
- [71] K. G. Larkin, "Reflections on shannon information: In search of a natural information-entropy for images," *arXiv preprint arXiv:1609.01117*, 2016.
- [72] A. Oliva and A. Torralba, "Modeling the shape of the scene: A holistic representation of the spatial envelope," *International Journal of Computer Vision*, vol. 42, no. 3, pp. 145–175, 2001.
- [73] N. Dalal and B. Triggs, "Histograms of oriented gradients for human detection," in *Computer Vision and Pattern Recognition*, 2005, pp. 886–893.
- [74] T. Ojala, M. Pietikainen, and T. Maenpaa, "Multiresolution gray-scale and rotation invariant texture classification with local binary patterns," *IEEE Transactions on Pattern Analysis and Machine Intelligence*, vol. 24, no. 7, pp. 971–987, 2002.
- [75] "Fgvc flowers dataset." [Online]. Available: <https://sites.google.com/view/fgvc5/competitions/fgvcx/flowers>
- [76] L. Bossard, M. Guillaumin, and L. J. V. Gool, "Food-101 mining discriminative components with random forests," *European Conference on Computer Vision*, vol. 8694, pp. 446–461, 2014.
- [77] B. Oreshkin, P. R. López, and A. Lacoste, "Tadam: Task dependent adaptive metric for improved few-shot learning," in *Neural Information Processing Systems*, 2018, pp. 721–731.
- [78] W. Min, S. Jiang, L. Liu, Y. Rui, and R. Jain, "A survey on food computing," *ACM Computing Surveys*, vol. 52, no. 5, p. 92, 2019.
- [79] N. Dvornik, C. Schmid, and J. Mairal, "Selecting relevant features from a universal representation for few-shot classification," in *European Conference on Computer Vision*, 2020, pp. 769–786.
- [80] C. P. Phoo and B. Hariharan, "Self-training for few-shot transfer across extreme task differences." *arXiv preprint arXiv:2010.07734*, 2020.
- [81] L. Tang, D. Wertheimer, and B. Hariharan, "Revisiting pose-normalization for fine-grained few-shot recognition," in *Computer Vision and Pattern Recognition*, 2020, pp. 14352–14361.
- [82] Y. Zhu, C. Liu, and S. Jiang, "Multi-attention meta learning for few-shot fine-grained image recognition," in *International Joint Conference on Artificial Intelligence*, 2020.
- [83] M. Ren, R. Liao, E. Fetaya, and R. Zemel, "Incremental few-shot learning with attention attractor networks," in *Neural Information Processing Systems*, 2019, pp. 5275–5285.
- [84] S. W. Yoon, J. Seo, D. Kim, and J. Moon, "Xtarnet: Learning to extract task-adaptive representation for incremental few-shot learning," in *International Conference on Machine Learning*, 2020.
- [85] X. Tao, X. Hong, X. Chang, S. Dong, X. Wei, and Y. Gong, "Few-shot class-incremental learning," in *Computer Vision and Pattern Recognition*, 2020, pp. 12183–12192.
- [86] Q. Liu, O. Majumder, A. Achille, A. Ravichandran, R. Bhotika, and S. Soatto, "Incremental few-shot meta-learning via indirect discriminant alignment." in *European Conference on Computer Vision*, 2020, pp. 685–701.
- [87] Y. Zhu, W. Min, and S. Jiang, "Attribute-guided feature learning for few-shot image recognition," *IEEE Transactions on Multimedia*, 2020.
- [88] P. Wang, L. Liu, C. Shen, Z. Huang, A. van den Hengel, and H. T. Shen, "Multi-attention network for one shot learning," in *Computer Vision and Pattern Recognition*, 2017, pp. 6212–6220.
- [89] Z. Peng, Z. Li, J. Zhang, Y. Li, G.-J. Qi, and J. Tang, "Few-shot image recognition with knowledge transfer," in *International Conference on Computer Vision*, 2019, pp. 441–449.
- [90] R. Chen, T. Chen, X. Hui, H. Wu, G. Li, and L. Lin, "Knowledge graph transfer network for few-shot recognition," *Association for the Advancement of Artificial Intelligence*, vol. 34, no. 7, pp. 10575–10582, 2020.
- [91] A. Li, T. Luo, Z. Lu, T. Xiang, and L. Wang, "Large-scale few-shot learning: Knowledge transfer with class hierarchy," in *Computer Vision and Pattern Recognition*, 2019, pp. 7212–7220.